

## Growth of step-free surfaces on device-size (0001)SiC mesas

J. Anthony Powell,<sup>a)</sup> Philip G. Neudeck, Andrew J. Trunek,<sup>b)</sup> Glenn M. Beheim, Lawrence G. Matus, Richard W. Hoffman, Jr.,<sup>c)</sup> and Luann J. Keys  
 NASA Glenn Research Center at Lewis Field, Cleveland, Ohio 44135

(Received 8 May 2000; accepted for publication 11 July 2000)

It is believed that atomic-scale surface steps cause defects in single-crystal films grown heteroepitaxially on SiC substrates. A method is described whereby surface steps can be grown out of existence on arrays of device-size mesas on commercial “on-axis” SiC wafers. Step-free mesas with dimensions up to 200  $\mu\text{m}$  square have been produced on 4H-SiC wafers and up to 50  $\mu\text{m}$  square on a 6H-SiC wafer. A limiting factor in scaling up the size and yield of the step-free mesas is the density of screw dislocations in the SiC wafers. The fundamental significance of this work is that it demonstrates that two-dimensional nucleation of SiC can be suppressed while carrying out step-flow growth on (0001)SiC. The application of this method should enable the realization of improved heteroepitaxially-grown SiC and GaN device structures. © 2000 American Institute of Physics. [S0003-6951(00)02636-X]

Single crystals of the hexagonal polytypes of silicon carbide (SiC) are being used as substrates for the growth of heteroepitaxial films. Important commercial applications include the growth of GaN on SiC for the fabrication of short-wavelength light emitting diodes, laser diodes, and heterojunction radio frequency transistors.<sup>1</sup> The GaN films contain a very high density of defects (typically  $10^9 \text{ cm}^{-2}$ ).<sup>2</sup> The polished surface of “on-axis” commercial SiC wafers, frequently used for heteroepitaxy, is usually within  $0.3^\circ$  of the (0001) basal plane. Previous work<sup>3–5</sup> indicates that surface steps due to the small tilt angle promote extended crystal defects in heteroepitaxial films grown on SiC. The work of Tanaka *et al.*<sup>3</sup> indicates that the defect density in AlN films grown on (0001)6H-SiC is much less in regions grown over terraces between steps compared to regions near the steps. In the case of 3C-SiC grown on 6H-SiC, surface steps lead to double-positioning boundaries in the 3C films.<sup>4</sup> Surface steps may also play a role in the nonideal electrical performance of SiC inversion-channel metal–oxide–semiconductor field effect transistors (MOSFETs).<sup>5</sup> In previous work to eliminate surface steps from GaAs substrates, Nishida and Kobayashi<sup>6</sup> achieved step-free 100- $\mu\text{m}$ -wide regions within openings in a SiO<sub>2</sub> mask on a GaAs substrate by suppressing two-dimensional (2D) nucleation during growth. This letter describes initial results of the implementation of a recently patented process for the growth of step-free SiC surfaces on device-size mesas.<sup>7</sup>

Figure 1 illustrates in a simplified fashion our process for achieving step-free SiC surfaces. Figure 1(a) illustrates the surface steps present on the initial on-axis wafer surface due to the small tilt angle between the basal plane and the polished surface. Commercially available on-axis SiC wafers have a high surface step density. An on-axis wafer with a typical  $0.3^\circ$  tilt angle (relative to the basal plane) will have

surface steps with a terrace width of 50 nm, assuming a 0.25 nm step height (the height of a SiC bilayer). The first step in the process is to etch an array of mesas on the SiC wafer top surface. Then homoepitaxial growth is carried out on the mesas under conditions (described in the next paragraph) that promote step-flow growth while at the same time suppressing 2D nucleation on the mesa tops. In this manner, the atomic steps on each mesa top grow themselves out of existence, leaving a basal plane surface (tilted with respect to the original surface), as illustrated in Fig. 1(b). In idealized conditions where 2D terrace nucleation is completely sup-

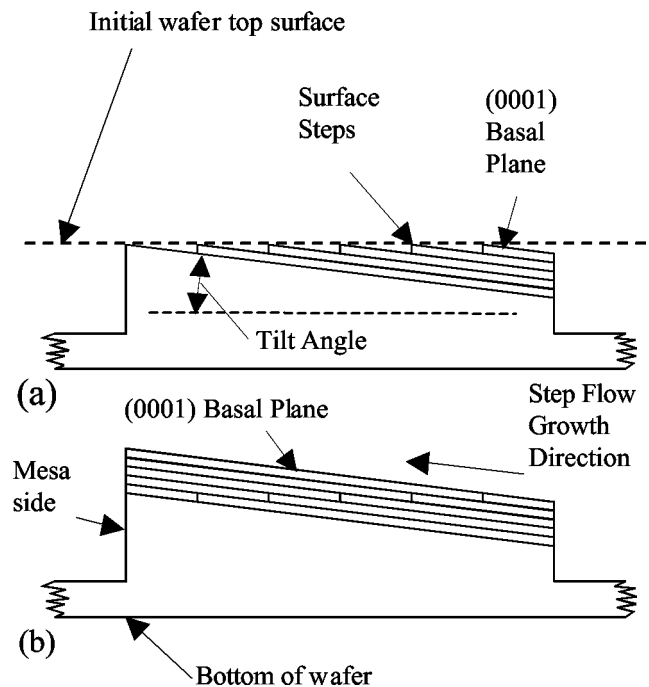


FIG. 1. Schematic diagram illustrating the growth of step-free mesas. (a) Before growth, initial mesa surface (parallel to bottom of wafer surface) contains steps due to tilt of basal plane with respect to polished wafer surface. (b) After growth, steps have been grown out of existence, leaving a step-free mesa surface parallel to the basal plane (i.e., tilted with respect to the initial surface).

<sup>a)</sup>Electronic mail: japowell@grc.nasa.gov

<sup>b)</sup>Present address: Akima Corporation, Fairview Park, OH 44126.

<sup>c)</sup>Also at: Ohio Aerospace Institute, Cleveland, OH 44135; present address: Emcore Corporation, Somerset, NJ 08873.

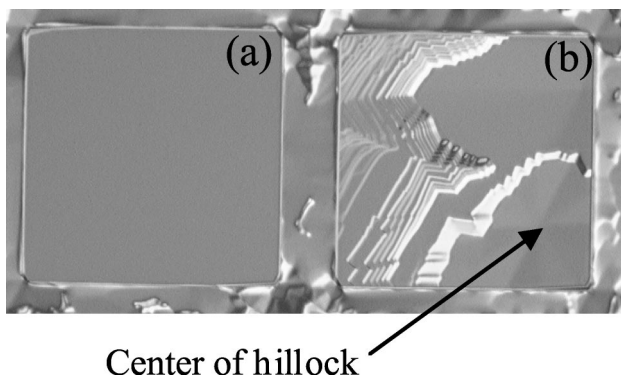


FIG. 2. Optical (Nomarski) images of two adjacent  $200\ \mu\text{m}$  square mesas on a 4H-SiC wafer. Mesa (a) (left) is step-free and mesa (b) (right) contains a screw dislocation which provided a continuous source of steps during growth.

pressed, there will be no further growth perpendicular to the basal plane. For simplicity, growth that occurs on the mesa sidewall and bottom of the grooves is not shown in Fig. 1(b).

To demonstrate the process, three commercially purchased on-axis SiC wafers were used (two 4H and one 6H). On the polished Si face of each wafer, mesas were fabricated by etching  $5\ \mu\text{m}$  deep grooves using an inductively coupled plasma etch system.<sup>8</sup> The indium tin oxide mesa mask contained square mesa patterns with the sizes  $50$ ,  $100$ ,  $200$ ,  $300$ , and  $400\ \mu\text{m}$ . The epitaxial growth was carried out in a commercial single-wafer chemical vapor deposition system with an inductively heated uncoated graphite susceptor.<sup>9</sup> Each wafer separately underwent an epitaxial growth process consisting of (1) an *in situ*  $\text{H}_2$  etch for 5 min at  $1600\ ^\circ\text{C}$  at a pressure of 100 mbar followed by (2) a growth for 30 min at  $1600\ ^\circ\text{C}$  at a pressure of 200 mbar. The sources of Si and C were  $\text{SiH}_4$  ( $2.7\ \text{cm}^3/\text{min}$ ) and  $\text{C}_3\text{H}_8$  ( $0.3\ \text{cm}^3/\text{min}$ ), respectively, in  $\text{H}_2$  (total flow  $4400\ \text{cm}^3/\text{min}$ ). Neither the etch nor the epitaxial growth parameters were optimized.

Following growth runs, the three SiC wafer surfaces were examined optically (Nomarski differential interference contrast) and by atomic force microscopy (AFM).<sup>10</sup> Growth was observed on the mesa tops and sidewalls as well as the bottom of the grooves. All three wafers exhibited step-free mesas; however, one of the two 4H wafers yielded a higher percentage of step-free mesas than the other two wafers. From the optical observations, nearly all of the mesa top surfaces on the 4H wafers exhibited one of three characteristics: (1) the surface was featureless, (2) the surface contained at least one hexagonal hillock which dominated the growth morphology, or (3) for a small percentage of mesas there were several large featureless regions separated by lines. For an unknown reason, hillocks were more difficult to discern with the optical microscope on the 6H mesa surfaces, compared with the 4H mesas; however, using moderate magnification (e.g.,  $100\times$ ), hillocks could be discerned on surfaces of both polytypes.

For the better of the two 4H wafers, most of the  $50$  and  $100\ \mu\text{m}$  mesas were optically featureless. All of the  $300$  and  $400\ \mu\text{m}$  mesas contained at least one hillock. Although most  $200\ \mu\text{m}$  mesas contained hillocks, there were tens of these mesas over the whole  $50\ \text{mm}$  wafer that were featureless. Figure 2 is an optical image of a 4H wafer showing two adjacent  $200\ \mu\text{m}$  mesas. Mesa (a) on the left is featureless

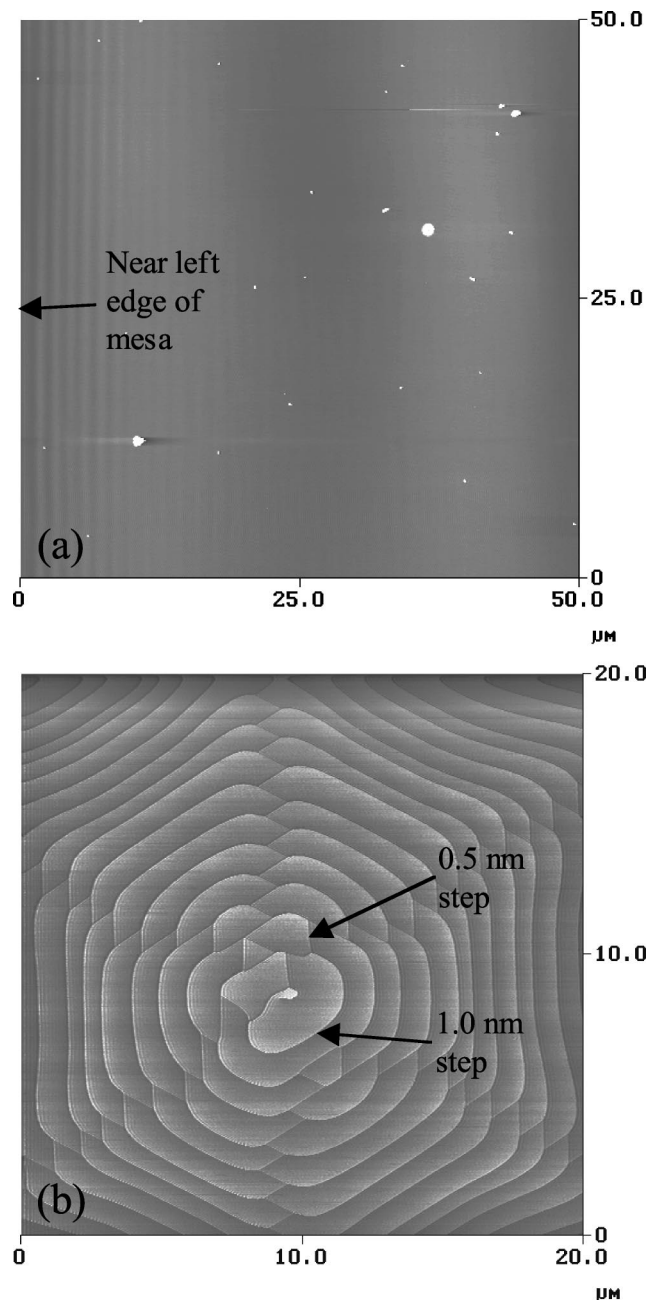


FIG. 3. AFM images of the two mesas of Fig. 2. (a)  $50\ \mu\text{m}$  scan near the left edge of step-free mesa A. (b)  $30\ \mu\text{m}$  scan of steps emanating from center of the screw dislocation in mesa B. Images have been “flattened” in order to show steps across entire scanned area. White “dots” are particles on surface.

and mesa (b) on the right contains a hillock which dominates the surface morphology.

AFM scans of the two  $200\ \mu\text{m}$  mesas of Fig. 2 are presented in Fig. 3. Figure 3(a) is one of sixteen  $50\ \mu\text{m}$  square scans of mesa (a) that were recorded in order to cover the entire  $200\ \mu\text{m}$  square mesa. No atomic steps or other features were observed in any of the 16 scans. Some parallel lines were observed in the scans at the left and right sides of the mesa, but these were attributed to artifacts of the measurement. This conclusion was reached since the parallel lines remained along the left and right sides of the AFM image even when the sample was rotated  $90^\circ$  (i.e., the lines did not follow the rotation of the sample). Such interference effects have been reported by other AFM users while observ-

ing extremely flat surfaces.<sup>11</sup> In this particular case, it appears that the interference fringes were mostly due to the mesa edge.

Figure 3(b) shows the center of the hillock of mesa (b). The well-defined steps (0.5 and 1.0 nm high) seen in this image, emanating from the center, are produced by a screw dislocation. The morphology and step height measurement indicates a screw dislocation with a 1 nm Burgers vector in the *c*-axis direction. This is consistent with an elementary screw dislocation in 4H-SiC.<sup>12</sup> Since the smallest step possible on a (0001) SiC surface is the height of a single bilayer (0.25 nm), it is clear that the AFM can detect any steps that may be present on the mesas.

Additional AFM scans (30  $\mu\text{m}$  square) were recorded for twenty-two 50  $\mu\text{m}$  mesas on the better 4H wafer. Hilllocks had been observed on only two of these mesas by the optical microscope; the remaining were optically featureless. The AFM scans confirmed that each of the two mesas with hillocks had steps due to screw dislocations, and of the remaining 20 optically featureless mesas, 18 were totally step-free while two mesas each had large step-free areas separated by stepped boundaries.

Examination of the 6H wafer yielded the following result. The only optically "featureless" mesas were a small percentage of the 50  $\mu\text{m}$  mesas. An AFM examination of 8 of these featureless 50  $\mu\text{m}$  mesas demonstrated that seven were step-free. An examination of 12 randomly selected 50  $\mu\text{m}$  mesas yielded only one step-free mesa. Most of the remaining 11 had hillocks generated by elementary screw dislocations, with step heights of 0.75 and 1.5 nm.

Some comments and conclusions from the previously mentioned observations are the following. It appears that the major determining factor in obtaining a step-free mesa was whether the mesa contained a screw dislocation. In almost every case, if a mesa contained a screw dislocation, then (1) *existing* surface steps (created by the off-cut tilt angle) would be grown out of existence by step-flow growth, and (2) *new* steps would be generated by the screw dislocation. The new steps dominate the mesa morphology. It had been expected that contamination and defects generated by polishing damage would play a greater role in determining mesa morphology. We conclude that the maximum size and yield of step-free mesas on a wafer is primarily limited by the density of screw dislocations in the wafer. For example, a uniform screw dislocation density of  $10^4 \text{ cm}^{-2}$  would produce an average of one dislocation for each 100  $\mu\text{m}$  square ( $10^{-4} \text{ cm}^2$  area) mesa. Based on the high yield of step-free 100  $\mu\text{m}$  square mesas on the better of the two 4H wafers, the dislocation density in that wafer is estimated to be less than  $10^4 \text{ cm}^{-2}$ . The dislocation density in the 6H wafer appears to be much higher than  $10^4 \text{ cm}^{-2}$ . We do not know whether this higher dislocation density is typical of commercially available 6H wafers.

The process described in this letter provides step-free mesa surfaces that are isolated from mesas with steps associated with screw dislocations. Hence, the step-free 100 and 200  $\mu\text{m}$  square mesas that can be produced will be very useful in evaluating the suitability of step-free SiC surfaces for the heteroepitaxial growth of low-defect single-crystal films of wide-band gap semiconductor compounds such as

3C-SiC, AlN, and GaN. If greatly improved wide-band gap heteroepitaxy can be realized on these step free surfaces, this in turn may enable new and/or greatly improved wide-band gap device structures, ranging from better-performing 3C-SiC diodes and transistors to previously unrealizable heterojunction FET and heterojunction bipolar transistor devices based on (Al)GaN/SiC and/or beta-SiC/alpha-SiC heterojunctions. One can also speculate that step-free SiC surfaces may enable fabrication of SiC MOSFETs and Schottky diodes with greatly reduced interface surface roughness, which may lead to improved device performance and reliability. The high yield achieved for the 100  $\mu\text{m}$  square mesas is dependent on the *area* of the mesa. One should be able to obtain a high yield for other mesa shapes of equivalent area; for example, a 20  $\mu\text{m} \times 500 \mu\text{m}$  mesa. Hence, the present yield should allow fabrication of laser diode structures<sup>1</sup> and other semiconductor devices with arbitrary shapes.

In summary, this letter reports initial results of an implementation of what we believe to be a potentially very useful crystal growth process. Step-free mesa surfaces were achieved in the three independent growth runs that were carried out. We have demonstrated that growth conditions exist for SiC that allow for step-flow growth while at the same time suppressing 2D terrace nucleation over a large step-free area. Experiments to optimize and understand the full window of effective growth conditions have not yet been carried out. However, we believe that conditions favorable to achieving epitaxial growth of step-free surfaces will include higher growth temperatures, and lower Si and C concentrations. Future work will also be directed toward more fully characterizing the polytypic composition and defect nature of the mesa surfaces using techniques that include cross-sectional transmission electron microscopy<sup>3</sup> and oxidation "color mapping."<sup>4</sup>

The authors gratefully acknowledge the assistance of Dr. P. Abel, C. Salupo, J. Krotine, and J. Heisler of the NASA Glenn Research Center.

<sup>1</sup>J. Edmond, G. Bulman, H. S. Kong, M. Leonard, K. Doverspike, W. Weeks, J. Niccum, S. T. Sheppard, G. Negley, D. Slater, J. D. Brown, J. T. Swindell, T. Overocker, J. F. Schetzina, Y.-K. Song, M. Kuball, and A. Nurmikko, in *International Conference on Silicon Carbide and Related Materials, 1997*, edited by G. Pensl, H. Morkoc, B. Monemar, and E. Janzen (Trans Tech, Stockholm, Sweden, 1998), Vol. 264–268, pp. 1421–1424.

<sup>2</sup>A. D. Hanser and R. F. Davis, in *Gallium Nitride and Related Semiconductors*, edited by J. H. Edgar, S. Strite, I. Akasaki, H. Amano, and C. Wetzel (Short Run, Exeter, 1999), pp. 386–390.

<sup>3</sup>S. Tanaka, R. S. Kern, and R. F. Davis, *Appl. Phys. Lett.* **66**, 37 (1995).

<sup>4</sup>J. A. Powell, J. B. Petit, J. H. Edgar, I. G. Jenkins, L. G. Matus, J. W. Yang, P. Pirouz, W. J. Choyke, L. Clemen, and M. Yoganathan, *Appl. Phys. Lett.* **59**, 333 (1991).

<sup>5</sup>T. Ouisse, *Phys. Status Solidi A* **162**, 339 (1997).

<sup>6</sup>T. Nishida and N. Kobayashi, *Jpn. J. Appl. Phys., Part 2* **37**, L13 (1998).

<sup>7</sup>J. A. Powell, D. J. Larkin, P. G. Neudeck, and L. G. Matus, US Patent No. 5,915,194 (June 22, 1999).

<sup>8</sup>G. M. Beheim and C. S. Salupo, *Mater. Res. Soc. Symp. Proc.* (to be published).

<sup>9</sup>Aixtron Inc. Model AIX 200/4 HT.

<sup>10</sup>Digital Instruments Model Dimension 3000.

<sup>11</sup>D. A. Chernoff and S. Magonov (unpublished).

<sup>12</sup>W. Si, M. Dudley, R. Glass, V. Tsvetkov, and C. H. Carter, Jr., *J. Electron. Mater.* **26**, 128 (1997).